Separation of Mixtures of Zeolites and Amorphous Materials and Mixtures of Zeolites with Different Pore Sizes into Pure Phases with the Aid of Cationic Surfactants

Han-Ju Lee, Yong Soo Park, Tae Sang Kim, Yun-Jo Lee, and Kyung Byung Yoon*

Center for Microcrystal Assembly and Department of Chemistry, Sogang University, Seoul 121-742, Korea

Received February 12, 2002. Revised Manuscript Received May 1, 2002

Upon shaking for 3 min at the proper concentrations, surfactant solutions of *n*-alkylpyridinium iodide ($C_nP^+I^-$, $n = 16$, 12, 10, and 8) readily develop very fine (<1 mm) and stable froth in the presence of zeolite crystals such as zeolite-A (A), mordenite (MOR), and zeolite-Y (Y) exchanged with M^{n+} ($M^{n+} = Na^+$, K^+, Ca^{2+}, or NH_4^+) as the charge-balancing cations. The frothy solution subsequently undergoes phase separation within 30 min into a top layer of thick froth and an underlying clear solution. Most of the zeolite particles are captured in the froth, and isolation of them is readily achieved by physical separation of the froth from the solution, followed by washing of the froth with ethanol. The recovered yield increases with increasing concentration of each surfactant and reaches a maximum (of greater than ∼90%) at a concentration that is slightly lower than the critical micelle concentration (CMC). The yield quickly decreases to a minimum (<20%) as the concentration passes the CMC. This phenomenon is attributed to the formation of hemimicelles and admicelles on the zeolite surfaces at concentrations below and above the CMC, respectively. In contrast, silica gel and alumina do not float under the same conditions. By using these two contrasting facts, the separation of mixtures of zeolites and silica or zeolites and alumina into each component is readily achieved. Interestingly, whereas the exchange of M^{n+} with C_nP^+ preferentially occurs with ions residing on the external surfaces of MOR and Y, the exchange occurs selectively with the interior cations when H^+ is the charge-balancing cation. As a result, HMOR and HY remain hydrophilic, and hence, they do not float even when the degree of exchange of H^+ with C_nP^+ reaches 13 and 15%, respectively. Consequently, the separation of mixtures of HMOR and HY is readily achieved by employing *n*-dodecylquinolinium iodide as the surfactant, which is size-excluded by HMOR but readily admitted into the interior of HY. The viability of the separation methods is demonstrated through the facile separations of autogenous mixtures of high-silica NaY and silica and zeolite-L and an unknown coproduced zeolite into each pure species.

Introduction

Zeolites are metastable, kinetic products.[1−4] Accordingly, they readily transform into thermodynamically more stable species even upon slight variation of the reaction conditions such as reaction temperature, time, impurities, order of reagent mixing, relative composition of reagents, nature of stirring, etc.[1−6] As a result, the production of mixed zeolite phases is very common, and it is fair to say that almost all zeolite syntheses result in the production of mixtures of zeolites with varying degrees of relative composition. Surprisingly, however, even though zeolite synthesis has been extensively investigated during the past five decades, there are no existing methods for separating zeolite mixtures into their pure components. For instance, none of the leading references[1−4] on zeolite synthesis either features a chapter dedicated to the separation of zeolite mixtures or even comments on the possible approaches to the separation of a desired zeolite species from mixtures. In this regard, the general practice has been to attempt, from the beginning, to produce the purest possible species, rather than wasting time by attempting the separation of mixtures into individual phases.

There are also cases in which a large excess of silica or another silicon source must be introduced into the synthesis gel with the intention of producing zeolites with high silicon contents[7] and controlled morphology.[8]

(1) Breck, D. W. *Zeolite Molecular Sieves*; John Wiley & Sons: New York, 1974; Chapter 4.
(2) Barrer, R. M. *Hydrothermal Chemistry of Zeolites*; Academic Press: London, 1982; Chapter 4.
(3) Dyer, A. *An Introduction to Zeolite Molecular Sieves*; John Wiley & Sons: New York, 1988; Chapter 5.
(4) Szostak, R. *Molecular Sieves: Principles of Synthesis and Identification*; Van Nostrand Reinhold: New York, 1989.
(5) Kostinko, J. A. In *Intrazeolite Chemistry*; Stucky, G. D., Dwyer, F. G., Eds.; ACS Symposium Series 218; American Chemical Society: Washington, DC, 1983; pp 3−19.
(6) Szostak, R. *Handbook of Molecular Sieves*; Van Nostrand Reinhold: New York, 1992; p 276.

10.1021/cm0202097 CCC: $22.00
Published on Web 07/23/2002

In such cases, the residual silica gel that coprecipitates with the desired zeolites should be removed after the reaction is completed. The removal of excess silica is usually accomplished by selectively dissolving the silica through repeated washing of the reaction mixture with large volumes of dilute aqueous sodium hydroxide solutions,[9] which is usually very time-consuming (several days or longer) and environmentally unfriendly. Care must also be taken not to increase the pH of the basic solution too much, as highly basic solutions readily dissolve even zeolite crystals. In this case, again, there are no alternatives that are more efficient, less time-consuming, and environmentally benign.

Natural zeolites are also commonly found in the form of mixtures with other types of zeolites and with nonporous minerals such as feldspars, silicas, clays, transition metal oxides, and organic contaminants.[10,11] Unless they are found in the form of large crystals,[11] the isolation of a single species from mixtures of very fine insoluble powders is a very difficult task. Therefore, for more efficient isolation and characterization of natural zeolites, it is also necessary to develop methods for separating zeolite mixtures and mixtures of zeolites with nonporous materials into pure individual components.

Surfactants have been widely employed as separating agents in various fields. One well-established example of surfactant-based separation is the froth flotation of ores.[12−20] The basic principle underlying froth flotation is that hydrophobicity is selectively imparted to the desired particles through the selective adsorption of the polar ends of the amphiphilic surfactant molecules onto the surfaces of the desired minerals in the mixtures and the hydrophobized particles are levitated to the top of the aqueous solution with the aid of air bubbles. The subsequent physical separation of the hydrophobic froth from the underlying aqueous solution retaining the hydrophilic material completes the separation.

The efficiency of flotation strongly depends on the concentration of surfactant. For instance, when the concentration of surfactant is lower than the critical micelle concentration (CMC), monolayers of surfactants, often called hemimicelles, cover the surfaces of particles. On the other hand, when the concentration is equal to or greater than CMC, patchy bilayers of surfactants, often called admicelles, cover the surfaces of the particles.[12,14,19,21−34] The particles covered with hemimicelles are hydrophobic and, hence, readily attach to the rising air bubbles upon contact. In contrast, the particles covered with admicelles are hydrophilic because of the polar ends of the second-layer surfactant molecules pointing outward. Hence, the particles remain in aqueous solution. The extension of this principle to the flotation of silica particles has received considerable interest.[18−21]

Surfactants have also been employed for groundwater treatment and the remediation of the contaminated soil.[28−36] Along these lines, growing attention has been paid to the modification of zeolite surfaces with various surfactant molecules because of the exceptional efficiency of zeolites modified with admicelles in the remediation of contaminated soil.[28−34] However, the possible application of surfactants in the separations of mixtures of zeolites into individual components and of zeolites from nonporous particles has not yet been attempted. The present work reports a novel method for separating zeolites from nonporous particles such as silica and alumina and for separating mixtures of zeolites into their individual components based on the zeolite pore sizes with the aid of cationic surfactants.

Experimental Section

Materials. Zeolite-A (Union Carbide 4A, lot 94279710013), mordenite (Union Carbide LZM-5, lot 962487061003-S), and zeolite-Y (Union Carbide LZY-52, lot 968087061020-S) in their Na^+-exchanged forms were treated with aqueous 1 M NaCl solution and subsequently washed with distilled deionized water until the silver ion test for chloride was negative. For

(7) Breck, D. W. U.S. Patent 3,130,007, 1964.
(8) For instance, perfect cubic zeolite-A crystals with almost no twined crystals are prepared by the introduction of a large excess of the silicon source into a gel consisting of $Si(OCH_2CH_3)_4$, $Al[OCH(CH_3)_2]_3$, $N(CH_3)_4OH$, NaCl, and H_2O in a molar ratio of 1:0.23:0.62:0.25:100.
(9) Jansen, J. C. In *Introduction to Zeolite Science and Practice*; Bekkum, H. V., Flanigen, E. M., Jansen, J. C., Eds.; Studies in Surface and Catalysis Series; Elsevier: Amsterdam, 1991; Vol. 58, p 107.
(10) Tschernich, R. W. *Zeolite of the World*; Geoscience Press: Phoenix, AZ, 1992; pp 27−31.
(11) Tsitsishvili, G. V.; Andronikashvili, T. G.; Kirov, G. N.; Filizova, L. D. *Natural Zeolites*; Ellis Horwood: New York, 1992; pp 93−95.
(12) Scamehorn, J. F.; Harwell, J. H. In *Surfactant-Based Separations—Science and Technology*; Scamehorn, J. F., Harwell, J. H., Eds.; ACS Symposium Series 740; American Chemical Society: Washington, DC, 2000; Chapter 1.
(13) Grieves, R. B.; Bhattacharyya, D. *Nature* **1965**, *207*, 476.
(14) Scamehorn, J. F.; Harwell, J. H. In *Surfactants in Chemical/Process Engineering*; Wasan, D. T., Ginn, M. E., Shah, D. O., Eds.; Surfactant Science Series 28; Marcel Dekker: NewYork, 1988; pp 98−106.
(15) Somasundaran, P.; Ramachandran, R. In *Surfactants in Chemical/Process Engineering*; Wasan, D. T., Ginn, M. E., Shah, D. O., Eds.; Surfactant Science Series 28; Marcel Dekker: NewYork, 1988; p 195.
(16) Fuerstenau, D. W.; Harris, G. H.; Jia, R. In *Surfactant-Based Separations—Science and Technology*; Scamehorn, J. F., Harwell, J. H., Eds.; ACS Symposium Series 740; American Chemical Society: Washington, DC, 2000; Chapter 14.
(17) Mulleneers, H. A. E.; Koopal, L. K.; Swinkels, G. C. C.; Bruning, H.; Rulkens, W. H. *Colloids Surf. A* **1999**, *151*, 293.
(18) Alexandrova, L.; Pugh, R. J.; Tiberg, F.; Grigorov, L. *Langmuir* **1999**, *15*, 7464.
(19) Koopal, L. K.; Goloub, T.; Keizer, A.; Sidorova, M. P. *Colloids Surf. A* **1999**, *151*, 15.
(20) Bremmell, K. E.; Jameson, G. J.; Biggs, S. *Colloids Surf. A* **1999**, *146*, 75.
(21) Chen, Y. L.; Chen, S.; Frank, C.; Israelachvili, J. *J. Colloid Interface Sci.* **1992**, *153*, 244.
(22) Somasundaran, P.; Healy, T. W.; Fuerstenau, D. W. *J. Phys. Chem.* **1964**, *68*, 3562.
(23) Chernyshova, I. V.; Rao, K. H.; Vidyadhar, A.; Shchukarev, A. V. *Langmuir* **2000**, *16*, 8071.
(24) Fan, A.; Somasundaran, P.; Turro, N. J. *Langmuir* **1997**, *13*, 506. (b) Chandra, P.; Somasundaran, P.; Turro, N. J. *J. Colloid Interface Sci.* **1987**, *117*, 31.
(25) Somasundaran, P.; Fuerstenau, D. W. *J. Phys. Chem.* **1966**, *70*, 90.
(26) Nishimura, S.; Scales, P. J.; Biggs, S.; Healy, T. W. *Langmuir* **2000**, *16*, 690.
(27) Manne, S.; Gaub, H. E. *Science* **1995**, *270*, 1480.
(28) Li, Z. *Langmuir* **1999**, *15*, 6438.
(29) Li, Z.; Roy, S. J.; Zou, Y.; Bowman, R. S. *Environ. Sci. Technol.* **1998**, *32*, 2628.
(30) Li, Z.; Bowman, R. S. *Environ. Sci. Technol.* **1997**, *31*, 2407.
(31) Haggerty, G. M.; Bowman, R. S. *Environ. Sci. Technol.* **1994**, *28*, 452.
(32) Sullivan, E. J.; Hunter, D. B.; Bowman, R. S. *Environ. Sci. Technol.* **1998**, *32*, 1948.
(33) Li, Z.; Burt, T.; Bowman, R. S.; *Environ. Sci. Technol.* **2000**, *34*, 3756.
(34) Li, Z.; Jones, H. K.; Bowman, R. S.; Helferich, R. *Environ. Sci. Technol.* **1999**, *33*, 4326.
(35) Boyd, S. A.; Lee, J.-F.; Mortland, M. M. *Nature* **1988**, *333*, 345.
(36) Lee, J.-F.; Crum, J. R.; Boyd, S. A. *Environ. Sci. Technol.* **1989**, *23*, 1365.

convenience, the framework structures are hereafter designated as A, MOR, and Y, respectively. The Na^+- and H^+-exchanged zeolites are designated as NaA, NaMOR, and NaY and HMOR and H(*x*)Y (*x* = 59, 80, and 90, depending on the degree of ion exchange), respectively. The particle sizes of the zeolites are 5−10 μm. The effective window sizes of the zeolites are A, 4.2; MOR, 7.0 × 6.7; Y, 7.4; and L, 7.1 Å. HMOR and H(90)Y were prepared by ion exchange of Na^+ in the parent zeolites with NH_4^+ followed by calcination at 550 °C for 12 h. For this process, each type of zeolite (10 g) was introduced into an aqueous solution of NH_4NO_3 (0.5 M, 100 mL), and the slurry was shaken for 12 h at room temperature. After filtration, the filter cake was washed with copious amounts of distilled deionized water. The washed zeolite was then calcined at 550 °C for 12 h. The above procedure was repeated three times to achieve maximum ion exchange. Chemical analyses of the H^+-exchanged zeolites revealed that the degree of H^+ exchange corresponds to 100% for HMOR [$H_8(Al_8Si_{40}O_{96})\cdot 24H_2O$] and 90% for H(90)Y [$H_{49}Na_5(Al_{54}Si_{138}O_{384})\cdot 240H_2O$]. Y zeolites with lesser degrees of H^+ exchange were also prepared by reducing the number of the above H^+-exchange cycles to 2 and 1 to examine the effect of the degree of H^+ exchange on the amount of flotation. Chemical analyses revealed that the degrees of H^+ exchange were 80% for H(80)Y [$H_{43,}Na_{11}(Al_{54}Si_{138}O_{384})\cdot 240H_2O$] and 59% for H(59)Y [$H_{32}Na_{22}(Al_{54}Si_{138}O_{384})\cdot 240H_2O$]. Zeolites exchanged with K^+ and Ca^{2+} were prepared from the corresponding Na^+ forms (10 g each) by repeated (five times) ion exchange with 0.5 M KCl and $CaCl_2$ solutions (100 mL each), respectively. All zeolite samples were dried in an oven and stored in air to allow equilibration with atmospheric moisture. Silica and neutral alumina with average particle sizes of 20 μm were purchased from Merck and Aldrich, respectively. Autogenous mixtures of high-silica NaY mixed with coprecipitated silica were prepared according to the literature procedure.[7] A mixture of K^+-exchanged zeolite-L (KL) and an unknown zeolite was synthesized at 180 °C from a gel consisting of SiO_2, $AlK(SO_4)_2$, KOH, and H_2O in a mole ratio of 1:0.07:1.1:50, in which LUDOX (HS-40) was used as the source of SiO_2. The synthetic gel was kept still in the oven during synthesis. Protonation of the mixture of zeolite-L (HL) and the unknown zeolite was carried out by repeating the aforementioned cycle of NH_4^+ exchange/calcination five times. Analysis of the degree of H^+ exchange in L and the unknown zeolite was not attempted.

1-Iodooctane, 1-iododecane, 1-iodododecane, 1-iodohexadecane, quinoline, 4-cyanopyridine, and tributylamine were purchased from Aldrich and used as received. Pyridine was purchased from Junsei and was purified by simple distillation prior to use. *N*-Alkylpyridinium iodide with alkyl = *n*-octyl, *n*-decyl, *n*-dodecyl, and *n*-hexadecyl (designated as $C_8P^+I^-$, $C_{10}P^+I^-$, $C_{12}P^+I^-$, and $C_{16}P^+I^-$, respectively) were obtained by refluxing each acetonitrile (30 mL) solution of pyridine (1 g, 12 mmol) and the corresponding 1-iodoalkane (10 mmol). The obtained yellow salts were purified by repeated (>3 times) recrystallization from ethyl acetate and *n*-hexane. $C_8P^+I^-$: yield 95%, yellow solid, mp 39−40 °C. $C_{10}P^+I^-$: yield 95%, yellow solid, mp 73−74 °C. $C_{12}P^+I^-$: yield 96%, pale yellow solid, mp 84−85 °C. $C_{16}P^+I^-$: yield 98%, pale yellow solid, mp 95−96 °C. The iodide salts of *N*-dodecylquinolinium ($C_{12}Q^+I^-$), *N*-dodecyl(4-cyano)pyridinium ($C_{12}CP^+I^-$), and *N*-dodecyltributylammonium ($C_{12}TBA^+I^-$) were similarly prepared from quinoline (1.50 g, 12 mmol), 4-cyanopyridine (1.20 g, 12 mmol), and tributylamine (2.00 g, 11 mmol), respectively, by reaction with 1-iodododecane (2.96 g, 10 mmol). $C_{12}Q^+I^-$: yield 90%, fluorescent yellow solid, mp 84−85 °C. $C_{12}CP^+I^-$: yield 90%, yellow solid, mp 144−145 °C. $C_{12}TBA^+I^-$: yield 95%, white solid, mp 84−85 °C. *N*-Dodecyltrimethylammonium bromide ($C_{12}TMA^+Br^-$, TCI) and sodium dodecyl sulfate (SDS, Aldrich) were commercial products that were used as received. (See Supporting Information for the ^{1}H NMR data of the surfactant molecules synthesized in this work.)

Determination of the Amounts of Zeolites Floated and the Amounts of Surfactants Sorbed onto the Zeolites. Typically, an aliquot of zeolite-A (1 g) was introduced into a 125-mL pear-shaped separatory funnel containing an aqueous solution of $C_{12}P^+I^-$ (3 mM, 50 mL). After vigorous shaking for 3 min, the aqueous mixture was allowed to settle for 30 min. Gradually, the frothy solution underwent phase separation into a top layer of froth and a clear solution under the froth. The underlying clear solution was transferred into a flask by opening the stopcock at the bottom of the separatory funnel. Any zeolite particles that were retained in the clear solution were collected by centrifugation. The concentration of the surfactant in the particle-free clear solution was measured with a UV−vis spectrophotometer by taking an aliquot and diluting it to an appropriate concentration until the absorbance was less than 1 in the spectrum. In this way, the amount of surfactant sorbed (the amount removed from the solution to the zeolite by ion exchange and adsorption) onto the zeolite was estimated. The measured molar extinction coefficient for $C_{12}P^+$ was 4400 M^{-1} cm^{-1} at 259 nm (λ_{max}), which is slightly higher than the reported value.[19,37,38] The molar extinction coefficients for the related materials $C_8P^+I^-$, $C_{10}P^+I^-$, and $C_{16}P^+I^-$ were also the same.

To measure the weight of the zeolite contained in the froth, 15 mL of ethanol was introduced into the funnel containing the froth. This settles the froth into an ethanol suspension of zeolite particles. The zeolite suspension in ethanol was transferred into a test tube. The zeolite particles were then isolated by decanting the supernatant alcoholic solution after centrifugation of the heterogeneous mixture. The zeolite particles were further washed with fresh ethanol by repeating the centrifugation/decantation cycle. After washing, the zeolite particles were dried in an oven at 120 °C for 6 h. The weight of the zeolite particles was measured after they had been allowed absorb moisture from the atmosphere.

The above procedure was repeated with varying concentration of $C_{12}P^+I^-$ from 0.1 to 10 mM. In the cases where all or parts of zeolite crystals did not float because of unfavorable concentrations of the surfactant (at lower or higher concentrations), the zeolite particles at the bottom of the funnel were removed by draining the underlying aqueous solutions. Determination of the amounts of zeolites floated and the amounts of surfactant sorbed onto the zeolites was carried out similarly. The above procedure was employed for the flotation of other types of zeolite. The measured molar extinction coefficient of $C_{12}Q^+$ was 7600 M^{-1} cm^{-1} at 316 nm (λ_{max}), and this value was used for the determination of the amounts of surfactant sorbed onto HMOR and H(90)Y.

Separation of Zeolites from Silica Particles. This procedure is essentially the same as the above except that a larger (250-mL) separatory funnel charged with a larger amount (100 mL) of $C_{12}P^+I^-$ (3 mM) was employed and that a mixture of NaA and silica gel (1 g each) was introduced into the funnel. Another difference from the above procedure is that only half (50 mL) of the underlying aqueous solution containing the particles at the bottom of the funnel was transferred to a collecting flask after initial shaking and settling. Into the funnel containing the froth and the remaining half (50 mL) of the aqueous solution, 50 mL of fresh distilled deionized water was newly introduced, and the funnel was shaken once again for an additional 3 min. The rest of the procedure is the same as the above procedure. Each fraction of isolated particles was weighed, and the nature and morphology of each fraction were analyzed by scanning electron microscopy (SEM) and X-ray powder diffractometry, respectively. Separation of the autogenous mixture of high-silica NaY and the coprecipitated silica gel into each component was carried out similarly.

Separation of Zeolite Mixtures into Individual Components. As test cases, artificial 1:1 mixtures (by weight) of NaA/HMOR and HMOR/H(90)Y were prepared. The above standard procedure for the separation of zeolites from silica was employed similarly. $C_{12}P^+I^-$ (3 mM, 100 mL) was employed for the separations of NaA/HMOR (2 g) and the autogenous mixture of HL/H^+-exchanged unknown zeolite (2

(37) Brownawell, B. J.; Chen, H.; Collier, J. M.; Westall, J. C. *Environ. Sci. Technol.* **1990**, *24*, 1234.

(38) Goloub, T. P.; Koopal, L. K.; Bijsterbosch, B. H.; Sidorova, M. P. *Langmuir* **1996**, *12*, 3188.

g) into each component. $C_{12}Q^+I^-$ (5 mM, 100 mL) was used for the separation of HMOR/H(90)Y (2 g) into each component.

Contact Angle Measurements. For water contact angle measurements, 50 mg of each zeolite sample was pressed into a pellet with a diameter of 0.5 in. using an IR pelletizer at an applied pressure of 5 t cm^{-2}. The values were taken from three different regions 5 s after water was dropped onto the pellet surface. Six data points were obtained from two pellets, and the reported values represent the averages.

Instrumentation. Scanning electron microscope (SEM) images of zeolites were obtained with a FE-SEM (Hitachi S-4300) at an acceleration voltage of 20 kV. On top of the samples, platinum/palladium alloy (in the ratio of 8:2) was deposited with a thickness of about 15 nm. The chemical compositions of zeolites were obtained with a sequential X-ray fluorescence spectrometer (Shimaduz XRF-1700) located at the Inter-University Center for Natural Science Research Facilities. ^{1}H NMR spectra were recorded on a Varian Jemini 300 NMR spectrometer. The ^{13}C NMR spectrum of $C_{12}P^+I^-$ was recorded on a Varian Unity-Inova 500 instrument. Magic angle spinning ^{13}C solid-state NMR spectra of $C_{12}P^+$-exchanged H(90)Y and crystalline $C_{12}P^+I^-$ were recorded on a Bruker DSX 400 MHz spectrometer. UV−vis spectra of the samples were recorded on a Shimadzu UV-3101PC instrument. Water contact angles of the zeolite pellets were measured with a contact angle goniometer (Ramé-Hart model 100-00). Diffuse reflectance UV−vis spectra of solid samples were obtained using an integrating sphere. X-ray diffraction patterns were obtained with a Rigaku diffractometer (D/MAX-1C) with a monochromated beam of Cu Kα radiation.

Results and Discussion

Flotation of NaA with $C_nP^+I^-$ (n = 8, 10, 12, and 16). Taking $C_{12}P^+I^-$ as a prototypical surfactant, the surfactant solution suspended with NaA particles readily turned frothy during the 3-min shaking period in the concentration range from 0.1 to 3 mM. The thick frothy solution underwent phase separation into a top frothy layer and an underlying transparent solution during the 30-min settling period. Analysis of the froth showed that most of the zeolite particles were captured within the froth. Interestingly, the zeolite-containing froth was remarkably stable, and as a result, the thick froth retained most of its initial volume for several days when kept still. Another characteristic point to note is that the sizes of the bubbles in the froth were very small (<1 mm) and nearly uniform. In contrast, the zeolite-free surfactant solutions usually produced much larger bubbles with irregular sizes ranging from 1 mm to 1 cm. Furthermore, the zeolite-free bubbles were highly unstable; most of them quickly disappeared within a few minutes when kept still.

The volume of the fine froth increased as the amount of zeolite particles transferred into the froth increased. Simultaneously, the degree of transparency of the underlying aqueous solution increased as lesser amounts of zeolite particles were retained in the underlying solution. The amount of zeolite particles captured in the froth (and the apparent volume of the froth) gradually increased from 56 to 76, 90, and 100% with increasing concentration of $C_{12}P^+I^-$ from 0.1 to 0.5, 1, and 3 mM, respectively. However, at higher concentrations, the floated amount sharply decreased. Thus, the recovered amounts decreased from 100 to 84, 61, and 9% upon increasing concentration from 3 to 4, 5, and 6 mM, respectively. The concentration-dependent variation of the floated amounts of NaA for $C_nP^+I^-$ (n = 16, 12, 10, and 8) is shown in Figure 1A. The concentration at which the floated amount of NaA reached a maximum (denoted as C_{MF}) was 0.1, 3, 10, and 50 mM for each C_nP^+ with n = 16, 12, 10, and 8, respectively. Thus, C_{MF} gradually increased with decreasing chain length of C_nP^+. It is also interesting to note that each C_{MF} appears at a concentration that is slightly lower than the critical micelle concentration (CMC) of each surfactant, as independently marked in Figure 1A.[39,40]

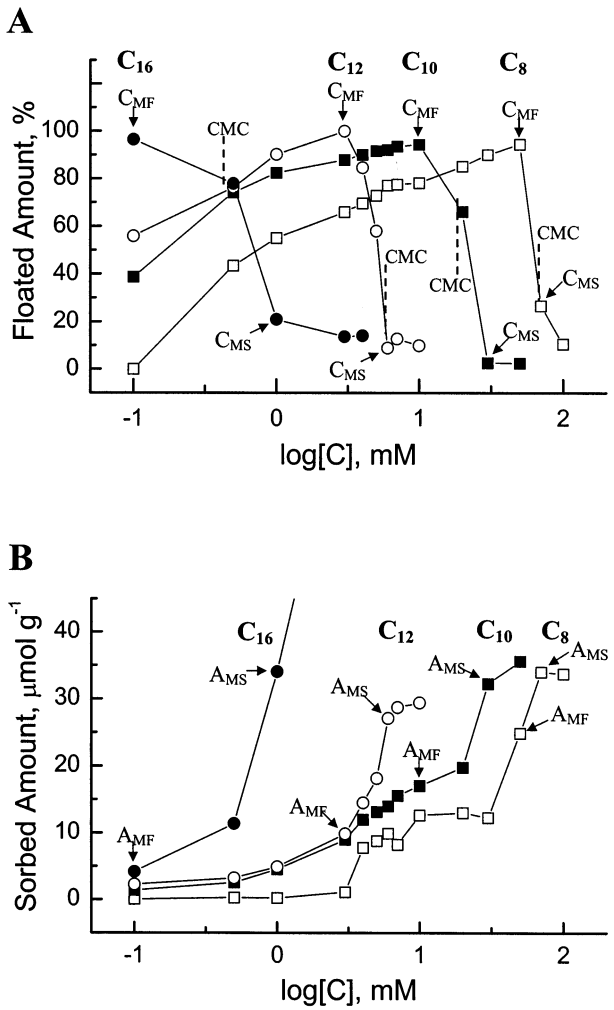

Figure 1. (A) Chain-length-dependent variation of the floated amount of NaA with increasing concentration of each surfactant and (B) progressive increase in the sorbed amount of each surfactant with increasing concentration. The concentration that gives rise to the maximum floated amount (C_{MF}), the lowest concentration that gives rise to the maximum sunken amount (C_{MS}), and the critical micelle concentration (CMC) for each surfactant are indicated in panel A, and the corresponding sorbed amounts at C_{MF} (A_{MF}) and C_{MS} (A_{MS}) are indicated in panel B.

The relationship between the concentration of the surfactant and the corresponding sorbed amount is plotted in Figure 1B. As marked in the figure, the sorbed

(39) The CMC values for $C_nP^+I^-$ used in this report are 0.4, 5.4, 18.9, and 66.2 mM for n = 16, 12, 10, and 8, respectively. The CMC values of $C_{16}P^+I^-$ and $C_{12}P^+I^-$ were taken from Perche, T.; Auvray, X.; Petipas, C.; Anthore, R.; Perez, E.; Rico-Lattes, I.; Lattes, A. *Langmuir* **1996**, *12*, 863, and the corresponding CMC values of $C_{10}P^+I^-$ and $C_8P^+I^-$ were estimated from the Klevens equation, log CMC = $A - Bn_c$, where A and B are constants and n_c represents the number of carbon atoms in the linear aliphatic chain. See ref 40.

(40) Jönsson, B.; Lindman, B.; Holmberg, K.; Kronberg, B. *Surfactants and Polymers in Aqueous Solution*; John Wiley & Sons: Chichester, U.K. 1998; p 37.

amount of each surfactant onto NaA at C_{MF} (denoted as A_{MF}) progressively increased with decreasing chain length in C_nP^+, i.e., $A_{MF} = 4.2$, 9.9, 17.0, and 24.9 μmol g^{-1} for $n = 16$, 12, 10, and 8, respectively. The sorbed amounts are primarily attributed to the amounts of surfactant cations exchanged onto the *external* surfaces of zeolite crystals on the basis of the following two facts. First, the kinetic diameter (5.9 Å)[41] of each surfactant molecule is larger than the size of the pore opening of NaA (4.2 Å). Second, the surfactant molecules do not form micelles in solution; hence, at concentrations below the CMC, admicelles do not adhere to the particle surfaces.[12,14,19,21−36] In support of the above interpretation, sodium dodecyl sulfate (SDS), an anionic surfactant, does not cause flotation of NaA particles, irrespective of the concentration. More convincingly, the UV−vis spectrophotometric analysis of the aqueous solution revealed that the concentration (amount) of iodide (monitored at ∼225 nm) stays the same whereas the concentration of $C_{12}P^+$ (monitored at ∼259 nm), a prototypically employed surfactant, keeps decreasing with increasing amount of NaA in the solution. Therefore, the above result unambiguously establishes that ion exchange proceeds between $C_{12}P^+$ and the Na^+ residing on the external surface of NaA at concentrations equal to and below C_{MF}. On the basis of the above result, we now conclude that the surfactant-induced incorporation of NaA into the froth occurs as a result of the hydrophobic interaction between the hydrophobic air bubbles and the alkyl chains of the surfactant ions exchanged onto the external surface of zeolite-A.

In terms of ion exchange, the A_{MF} values correspond to about 0.07, 0.18, 0.31, and 0.45% exchange of Na^+ with C_nP^+ for $n = 16$, 12, 10, and 8, respectively, with respect to the total available exchangeable sites of zeolite-A crystals, which were estimated on the basis of the unit cell composition. In the case of the NaA crystals employed in this study, the estimated amount of ion-exchangeable sites on the external surface actually corresponds to 0.45% of the total available sites.[42] This estimation is quite reasonable in the sense that the external surface areas of smaller (∼1 μm) zeolite crystals are ∼1% of the total surface area.[43] Accordingly, with respect to the number of the external exchangeable sites of the zeolite-A employed in this study, the degree of ion exchange of Na^+ with C_nP^+ on the external surface is estimated to be 16, 40, 69, and 100% for $n =$ 16, 12, 10, and 8, respectively. This result indicates that the minimum number of C_nP^+ ions required to induce NaA to float progressively decreases with increasing chain length of the surfactant. In other words, a smaller number of surfactant ions is required to impart a similar degree of hydrophobicity to zeolite-A particles with increasing hydrophobicity (chain length) of the surfactants.

As mentioned earlier, the floated amount of NaA decreased sharply when the concentration was increased above C_{MF}. The lowest concentration at which the sunken amount of NaA reaches a maximum is denoted C_{MS}. The C_{MS} values were 1, 6, 30, and 70 mM for $n = 16$, 12, 10, and 8, respectively. It is also interesting to note that each C_{MS} appeared at a concentration that was slightly higher than the corresponding CMC. Thus, with CMC as the turning point, the amount of zeolite crystals that float turns sharply from a maximum to a minimum with increasing concentration, irrespective of the chain length of C_nP^+. This phenomenon is very much likened to the general surfactant-induced flotation efficiencies of particles.[12,14,19,21−36]

The sorbed amount of each surfactant onto NaA at C_{MS} (denoted A_{MS}) corresponds to 34, 27, 32, and 34 μmol g^{-1} for $n = 16$, 12, 10, and 8, respectively. Thus, in contrast to the A_{MF} values, the A_{MS} values are nearly invariant. The estimation of the surface coverage of NaA in terms of ion exchange corresponds to 138, 109, 129, and 138% for $n = 16$, 12, 10, and 8, respectively, with respect to the total exchangeable sites on the external surface of zeolite-A crystals.

To interpret the occurrence of sorbed amounts larger than 100%, we imagined two possibilities. We first imagined the situation in which 100% of the total exchanged amount corresponds to the surfactant ions that fully cover the external surfaces of zeolite particles through ion exchange. The rest then corresponds to particles that form a bilayer with the first layer through hydrophobic interactions between the alkyl chains. If this is the case, then the degree of the bilayer coverage should correspond to 38, 9, 29, and 38% for $n = 16$, 12, 10, and 8, respectively. This, in turn, leads to the estimation that the remaining degree of monolayer coverage on the external surface of zeolite-A should correspond to 62, 91, 71, 62% for $n = 16$, 12, 10, and 8, respectively. If this were the case, then most of the zeolite-A should have floated for the three cases with $n = 16$, 12, and 10, as the results described earlier show that ∼100% of zeolite-A floats at monolayer coverages of 16, 40, and 69% for $n = 16$, 12, and 10, respectively. These conclusions contradict each other. Therefore, we conclude instead that the zeolite crystals are covered with admicelles when the sorbed amount reaches A_{MS}. The above conclusion is made based on the facts that micelles are formed in solutions above the CMC, each C_{MS} appears at a concentration higher than the CMC, and the A_{MS} values are too small to cover the whole zeolite surfaces uniformly with the bilayers.

Separation of an Artificial Mixture of NaA and Silica into Each Component. Knowing that C_nP^+ can induce flotation of nearly quantitative amounts of NaA from aqueous suspensions, we also examined the possibility of the flotation of silica and alumina, which have lower surface charge densities than NaA, especially at neutral conditions.[18−21] However, under our neutral conditions, the amorphous particles did not float at all, even at C_{MF} for each surfactant (see Table 1, last column). As a test case, we prepared an artificial 1:1 mixture of NaA and silica (by weight) and suspended the mixture in a surfactant solution where $C_{12}P^+I^-$ (3 mM, 100 mL) was employed as the prototypical surfactant. After applying the aforementioned procedure, we found that the heterogeneous mixture separated into three layers: a thick froth at the top, an underlying aqueous solution, and solid particles mostly sunken at the bottom of the separatory funnel. The X-ray powder diffraction pattern of each fraction (Figure 1 in the

(41) See ref 1, p 636.
(42) For the estimation, the morphology of zeolite-A was assumed to be perfectly cubic, and the measured (by SEM analysis) average length of each edge of the cubic zeolite-A crystal was 5 μm.
(43) See ref 1, p 595.

Table 1. Effect of the Nature of Surfactant on the Floated Amount of Each Zeolite with Different Framework Structure and Charge-Balancing Cation, Silica, and Alumina

surfactant type	[C][a]	zeolite					silica or alumina
		NaA	NaMOR	NaY	HMOR	HY	
$C_8P^+I^-$	50.0	94.3	85.3	89.2	00.0	00.0	00.0
$C_{10}P^+I^-$	10.0	94.2	89.1	90.9	00.0	00.0	00.0
$C_{12}P^+I^-$	3.0	99.9	85.8	88.8	00.0	00.0	00.0
$C_{16}P^+I^-$	0.1	96.5	90.4	86.6	00.0	00.0	00.0
$C_{12}CP^+I^-$	3.0	91.8	87.2	80.2	20.2	00.0	00.0
$C_{12}TMA^+Br^-$	3.0	95.3	87.2	86.1	38.4	00.0	00.0
$C_{12}Q^+I^-$	3.0	99.1	94.5	89.3	95.3	00.0	00.0
$C_{12}TBA^+I^-$	3.0	87.9	91.7	87.7	78.2	73.2	00.0
SDS	3.0	00.0	00.0	00.0	00.0	00.0	00.0

[a] In mM.

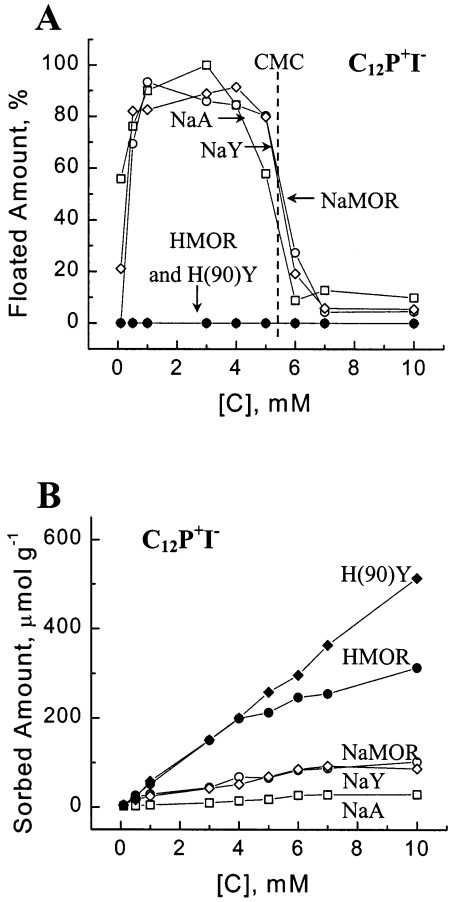

Figure 2. (A) Effect of the charge-balancing cation and type of zeolite on the floated amount of each zeolite and (B) corresponding amount of $C_{12}P^+$ sorbed onto each zeolite with increasing concentration of $C_{12}P^+I^-$.

Supporting Information) revealed that the particles in the froth and at the bottom of the funnel were pure zeolite-A and pure amorphous silica, respectively. The recovered yields were 83 and 79% for NaA and silica, respectively.

Flotation of NaMOR and NaY from the Corresponding Suspended Solution. Interestingly, the use of $C_nP^+I^-$ also readily induced flotation of NaMOR and NaY, despite the fact that their pore openings (see Table 1) are larger than the kinetic diameter of the surfactant (5.9 Å). Indeed, as demonstrated in Figure 2A, nearly quantitative amounts of NaMOR and NaY readily floated when $C_{12}P^+I^-$ was employed as the prototypical surfactant. This interesting result indicates that the surfactant cations are preferentially exchanged onto the external surfaces of zeolite particles. However, slightly larger concentrations of surfactant were required for the larger-pore zeolites to sink, as shown in Figure 2A, and hence, the sorbed amounts were always slightly larger than those of NaA (Figure 2B), which indicates that small fractions of the sorbed surfactants were simultaneously incorporated into the interior of the larger-pore zeolites.

Other related surfactants such as $C_{12}CP^+I^-$, $C_{12}TMA^+Br^-$, $C_{12}Q^+I^-$, and $C_{12}TBA^+I^-$ were also equally effective in inducing the flotation of NaA, NaMOR, and NaY, although there were minor variations in the floated amounts (see Table 1).[44] The surfactants also induced flotation of A, MOR, and Y exchanged with K^+, NH_3^+, and Ca^{2+} with similar efficiencies. In general, the degree of flotation decreased in the order $M^{n+}A > M^{n+}MOR > M^{n+}Y$, where M^{n+} denotes Na^+, K^+, NH_4^+, or Ca^{2+}. This order might arise because of the incorporation of increasing fractions of sorbed surfactant cations into the internal pores, as the pore size progressively increases in the reverse order. Consistent with this interpretation, the negatively charged surfactant SDS was not effective at all for floating M^{n+}-exchanged A, MOR, and Y.

Facile Ion Exchange of C_nP^+ Ions into the Interiors of H^+-Exchanged Zeolites. We discovered an interesting phenomenon that C_nP^+ do not induce flotation of HMOR and H(90)Y, as opposed to the corresponding M^{n+}-exchanged forms, even at concentrations that are highly effective for the flotation of M^{n+}-exchanged forms (see Table 1). In the case of Y, the floated amount of Y diminishes from 100 to 42, 8, and 0% with increasing degree of H^+ exchange from 0 to 59 [H(59)Y], 80 [H(80)Y], and 90% [H(90)Y], respectively, when $C_{12}P^+I^-$ is employed as a prototypical surfactant at a concentration of 3 mM. Thus, at least 90% exchange of H^+ is necessary to observe 0% flotation of the zeolite. To reach 90% exchange of H^+ in Y, repetition of the ion-exchange cycle three times was enough under our exchange conditions.

Figure 2A shows that H(90)Y did not respond to the surfactant through concentrations up to 10 mM, when $C_{12}P^+I^-$ was employed as the prototypical surfactant. Consistent with this result, the surfactant solution did not develop froth in the presence of HMOR or H(90)Y, as if no surfactant had been added to the solutions. Analysis showed that all of the surfactant molecules in the supernatant solutions were sorbed onto the HMOR and H(90)Y zeolites at concentrations lower than 4 mM (Figure 2B). Accordingly, there is a linear correlation between the amounts of $C_{12}P^+$ sorbed onto HMOR and H(90)Y and the concentration of the surfactant, as opposed to the amounts sorbed onto the corresponding Na^+-exchanged forms.

In the case of H(90)Y, which has larger pores, the proportionality between the concentration and the sorbed amount remained the same, even at concentrations higher than 4 mM, but this was not the case for HMOR with smaller pores. Analysis revealed that H(90)Y sorbed all of the added surfactant in the tested

(44) We did not attempt to obtain the corresponding C_{MF} for each surfactant but simply adjusted the concentration to 3 mM on the basis of fact that their chain lengths are the same as that of $C_{12}P^+I^-$.

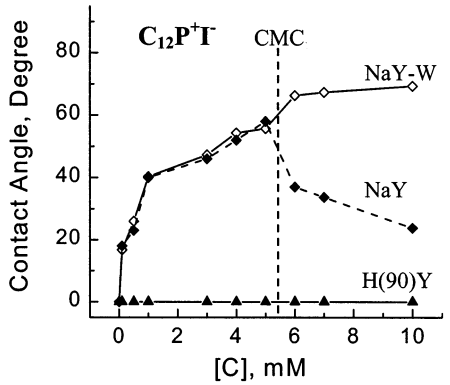

Figure 3. Water contact angles of pellets of NaY, NaY washed with ethanol (NaY−W), and H(90)Y (as indicated) that were prepared from the corresponding powders isolated from each solution of $C_{12}P^+I^-$ with increasing concentration. The CMC of the surfactant is also marked to show the abrupt change in the water contact angle of the NaY pellet upon passing this concentration.

concentrations up to 10 mM, whereas HMOR left some portions unsorbed. The amounts of $C_{12}P^+$ sorbed onto HMOR and H(90)Y at the highest tested concentration (10 mM) correspond to 312 and 500 μmol g^{-1}, respectively. These amounts, in turn, correspond to 13 and 15% of the total ion-exchangeable sites of HMOR and H(90)Y, respectively, so obviously, they are too large to be covered by the exchangeable sites placed only on the external surfaces of the zeolite crystals (<1%).

UV−vis spectrophotometric analyses of the supernatant solutions revealed that the concentration of iodide remained constant while all of the $C_{12}P^+$ molecules disappeared from the solutions in the presence of H(90)Y, for a $C_{12}P^+$ concentration of 3 mM. This result clearly establishes that $C_{12}P^+$ is the only species sorbed onto H(90)Y, but not I^-, the counteranion, which is a characteristic aspect of ion exchange.

The fact that the H^+-exchanged MOR and Y zeolites do not float regardless of the exchanged amounts of $C_{12}P^+$ (up to 312 and 500 μmol g^{-1}, respectively) strongly indicates that the H^+-exchanged zeolite particles remain hydrophilic regardless of the exchanged amounts. Consistent with this result, the independently measured water contact angles of the H(90)Y pellets (see Experimental Section) were invariably 0°, as illustrated in Figure 3, regardless of the amounts of $C_{12}P^+$ exchanged onto the zeolite from 1 to 500 μmol g^{-1}. In contrast, when the NaY pellets were prepared from the NaY particles recovered from the floated froth at C_{MF} (below the CMC), the water contact angle steeply increased, especially in the beginning as the sorbed amount of $C_{12}P^+$ increased. Above the CMC, however, the water contact angle started decreasing sharply, as shown in Figure 3. This phenomenon is consistent with the formation of admicelles on the external surfaces of the zeolites at concentrations above the CMC, as discussed earlier.

In contrast, the water contact angle continuously increased and finally reached a maximum of 75° when the pellets were made from material that was washed with ethanol prior to pelletization. This phenomenon can be interpreted as indicating that the ion-paired surfactants ($C_{12}P^+I^-$) residing within the surface-exchanged admicelles were readily removed by ethanol.

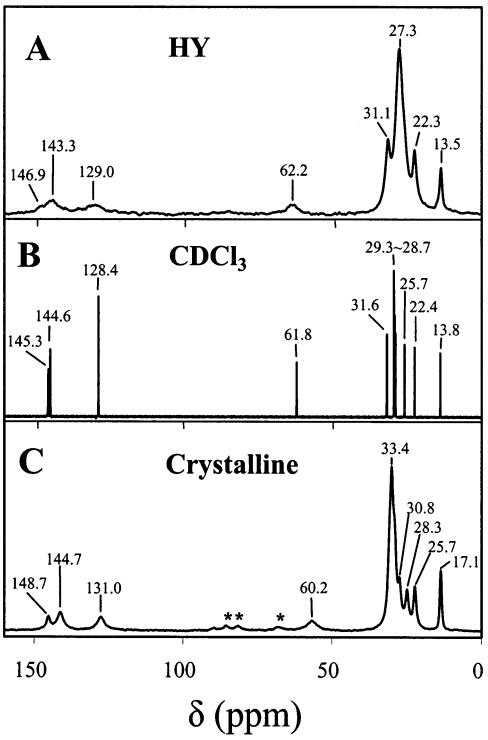

Figure 4. (A) Magic angle spinning solid-state ^{13}C NMR spectrum of $C_{12}P^+$-exchanged H(90)Y, (B) corresponding solution spectrum of $C_{12}P^+I^-$ in $CDCl_3$, and (C) solid-state spectrum of crystalline $C_{12}P^+I^-$. The peaks with asterisks in panel C represent the spinning sidebands.

Here, by ion-paired surfactants ($C_{12}P^+I^-$), we mean those that are supramolecularly adhered to the surface-exchanged surfactant ions ($C_{12}P^+$) in the surface-bound admicelles through hydrophobic interaction.

Thus, on the basis of the entirely different behaviors of H(90)Y than NaY, it is concluded that all of the $C_{12}P^+$ ions exchanged onto H(90)Y are pulled into the interior of H(90)Y, at least up to 500 μmol g^{-1}. A similar phenomenon is proposed to occur for HMOR with exchanged amounts of $C_{12}P^+$ up to 312 μmol g^{-1}. However, it still remains to be explained why such a dramatic difference arises upon changing the cation from M^{n+} to H^+.

One might alternatively suspect that the pyridine rings are cleaved from the alkyl tails by the surface acidic sites and, as a result, that only pyridine rings are sorbed into the interiors. As a means of clarifying this issue, we measured magic angle spinning ^{13}C solid-state NMR spectra of the H(90)Y that was treated with $C_{12}P^+I^-$ solution (10 mM), and compared the spectrum with that of crystalline $C_{12}P^+I^-$ and the ^{13}C NMR spectrum of the surfactant in solution ($CDCl_3$), as shown in Figure 4.

The resonance peaks at 129.0, 143.3, and 146.9 of H(90)Y (Figure 4A) clearly indicate the presence of the pyridinium moiety but not neutral pyridine in the species sorbed in H(90)Y. The peaks in the region of 13.5−31.1 show the presence of alkyl groups in the sorbed species. The peak at 62.2, which arises from the methylene group directly linked to the nitrogen of the pyridine ring, unambiguously indicates that the alkyl groups and the pyridinium moiety are interlinked through the methylene unit. The very close matching between the peak positions of the spectrum of H(90)Y

and the solution spectrum of authentic $C_{12}P^+I^-$ (Figure 4B) confirms that there are no species other than $C_{12}P^+$. This conclusion is further supported by the close agreement of the two relative intensity ratios between the peaks due to pyridinium and alkyl groups from H(90)Y and authentic crystalline $C_{12}P^+I^-$ (Figure 4C). Thus, the above NMR spectral evidence, coupled with the invariance of iodide absorption in the supernatant solution mentioned earlier, unambiguously verifies that $C_{12}P^+$ is indeed exchanged into the interior of HY. Interestingly, the peak positions of H(90)Y match more closely with those of the solution spectrum than those of crystalline $C_{12}P^+I^-$. This result further confirms that the $C_{12}P^+$ ions exist in the monomeric form in H(90)Y as in solution, rather than in the crystalline state and, as a corollary, that the resonance peaks of H(90)Y are not due to crystalline $C_{12}P^+I^-$ inadvertently present on the surface of the zeolite.

Separation of an Artificial Mixture of NaA and HMOR into Each Component. The above phenomenon prompted us to test whether it can be utilized to separate mixtures of zeolites consisting of zeolites exchanged with M^{n+} and H^+ into each component. As a test case, we first prepared a 1:1 mixture (by weight) of NaA and HMOR. Employing $C_{12}P^+I^-$ as the prototypical surfactant, we then introduced the mixture (2 g) into a separatory funnel containing the surfactant solution (3 mM, 100 mL) and shook the aqueous solution for 3 min. As a result, thick froth developed within the solution. Upon standing for 30 min, the frothy solution separated into three layers: a top layer of thick froth, a nearly transparent aqueous solution in the middle, and powders mostly sunken at the bottom of the funnel. The X-ray powder diffraction patterns of each fraction (Figure 2 in the Supporting Information) revealed that the floated particles were pure NaA and the particles that remained sunken at the bottom were pure HMOR. The recovered yields of the particles were 78 and 71% for NaA and HMOR, respectively. The above procedure represents a very simple yet highly efficient method for separating a zeolite mixture into each individual phase.

Pore-Size-Specific Separation of an Artificial Mixture of HMOR and H(90)Y into Each Component. We also tested related surfactants, namely, $C_{12}CP^+I^-$, $C_{12}TMA^+Br^-$, $C_{12}Q^+I^-$, and $C_{12}TBA^+I^-$, on HMOR and H(90)Y, and the results are tabulated in Table 1. The estimated kinetic diameters of the surfactant ions are 5.9,[41] 7.3,[45] 7.6,[46] and 8.1[41] Å, respectively. As mentioned earlier, the efficiencies of the surfactants in inducing flotation of $M^{n+}A$, $M^{n+}MOR$, and $M^{n+}Y$ are nearly the same as that of $C_nP^+I^-$ (see Table 1). However, the most striking difference is that these surfactants can also induce flotation of HMOR in amounts of 20.2, 38.4, 95.3, and 78.2%, respectively. Judging from the kinetic diameters alone, a linear correlation seems to exist between the floated amounts and the kinetic diameters. However, the ability of $C_{12}CP^+$ to induce flotation of HMOR, although in a small amount, is somewhat surprising because the kinetic diameter of the surfactant cation should be the same as that of $C_{12}P^+$. Apparently, the presence of a nitrile group in the aromatic ring seems to make a significant difference. The somewhat low yield (38.4%) in the floated amount with $C_{12}TMA^+Br^-$ as the surfactant, even though its kinetic diameter is larger than the size of the pore opening of MOR, is also difficult to interpret at this stage. Such discrepancies are likely to arise from the error margins in the estimation of the kinetic diameters of the surfactants. Nevertheless, the fact that $C_{12}TBA^+I^-$ can induce flotation of even H(90)Y in a large amount (73.2%) strongly supports the basic idea of this report that the exchange of the surfactant cations only on the external surface in the form of monolayers is responsible for flotation of zeolites, regardless of the countercation, either M^{n+} or H^+.

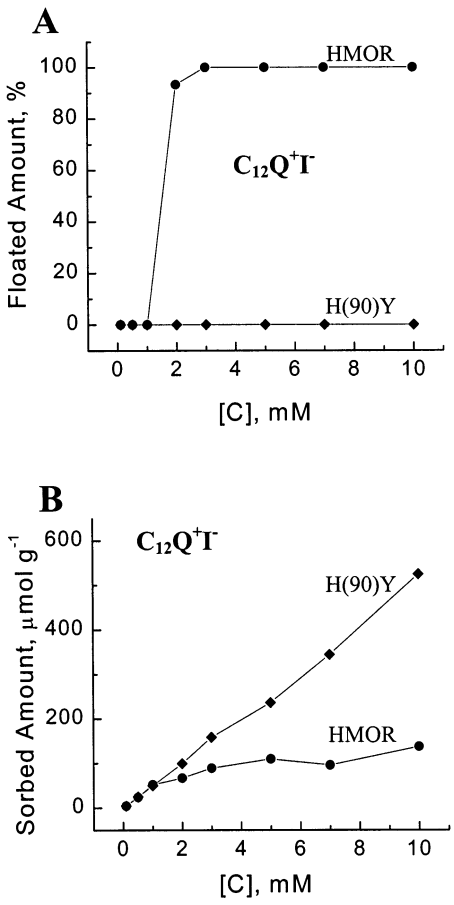

Figure 5. (A) Dramatic difference in the floated amount of HMOR and H(90)Y with employing $C_{12}Q^+I^-$ as the surfactant in the concentration range from 0.1 to 10 mM and (B) corresponding amount of $C_{12}Q^+$ sorbed onto each zeolite.

Among the surfactants tested in this report, $C_{12}Q^+I^-$ is unique because it exhibits a clear-cut difference in the floated amounts of HMOR and H(90)Y. Specifically, the surfactant-induced flotation of HMOR is essentially quantitative, but no flotation of H(90)Y occurs in the concentration range from 2 to 10 mM (Figure 5A). Consistent with this result, the amount of $C_{12}Q^+$ sorbed into H(90)Y continuously increased, whereas the amount sorbed into HMOR quickly reached a maximum at a small amount (~100 μmol g^{-1}), even at low concentrations (Figure 5B). The above unique property of $C_{12}Q^+$ also prompted us to attempt the separation of an artificial 1:1 mixture of HMOR and H(90)Y into each phase. By merely employing $C_{12}Q^+I^-$ as the surfactant

(45) See ref 1, p 70.

(46) Estimated from the easy access of the cation into the supercage of Y but not into the channels of MOR, coupled with the fact that this cation yields higher floated amounts of HMOR than $C_{12}TMA^+$ whose kinetic diameter has been estimated as 7.3 Å.

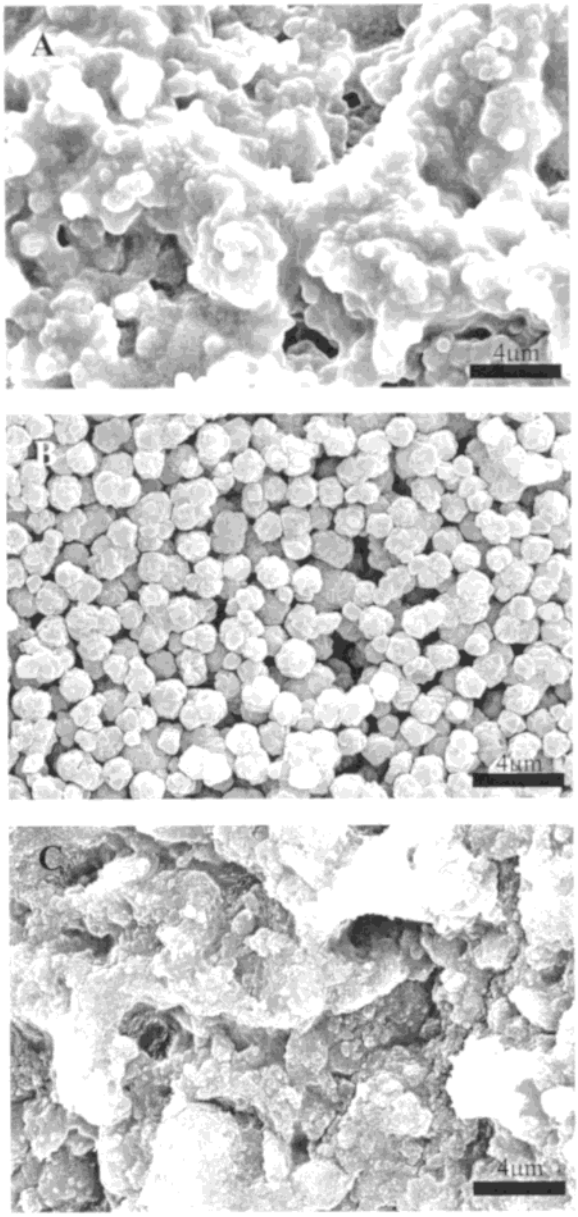

Figure 6. SEM images of (A) the mixture of NaY and silica, (B) the particles that floated, and (C) the particles that did not float.

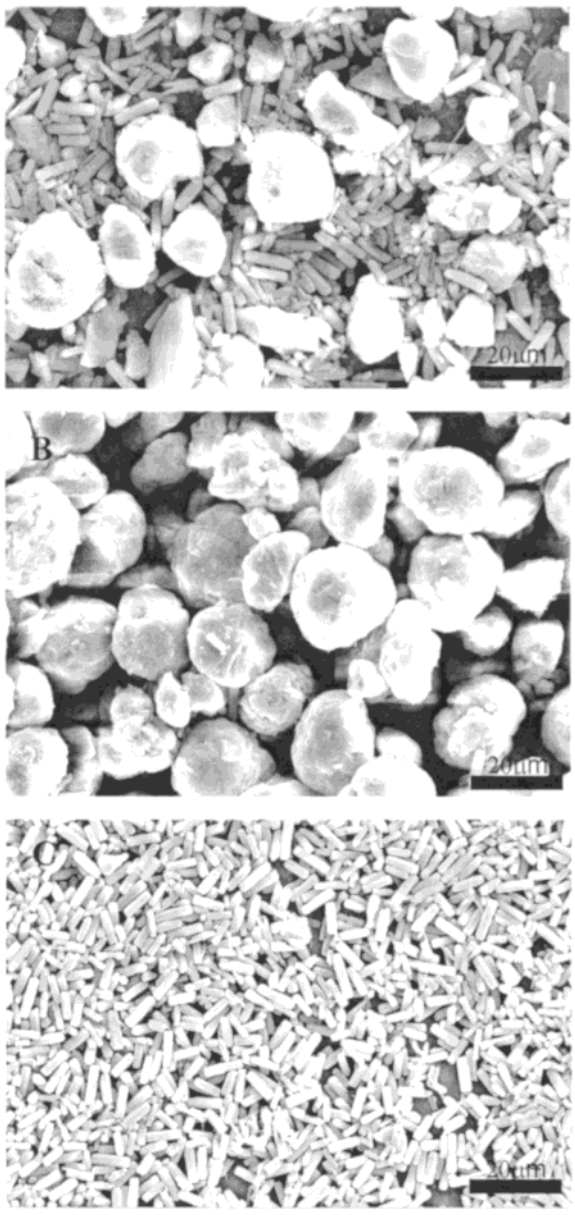

Figure 7. (A) SEM images of (A) the mixture of HL and an unknown zeolite, (B) the particles that floated, and (C) the particles that did not float.

and taking the aforementioned standard steps for the separation of the mixture, we also found that the mixture can be readily separated into pure HMOR and H(90)Y (see Figure 3 in the Supporting Information). The recovered yields were 87 and 74% for HMOR and H(90)Y, respectively.

Separation of an Autogenous Mixture of NaY and Silica into Each Component. As mentioned in the Introduction, a large excess of silica source is often introduced into the synthesis gel to increase the silicon content in the target zeolite. In such cases, large amounts of silica gel usually coprecipitate with the target zeolite. The silica gel has usually been removed by dissolving the products of the synthesis in dilute basic solutions. As mentioned earlier, the dissolution of excess silica with base is not desirable for many reasons. As a test case, we synthesized high-silica zeolite-Y according to the procedure of Breck et al.[7] using a large excess of the silicon source.[47] After 120 h of reaction, the mother liquor was removed by decantation. The residual solid phase was then washed twice with distilled deionized water. Indeed, the SEM image of the dried solid phase revealed that Y crystals were embedded within the dump of silica gel, as shown in Figure 6A. We then applied our standard procedure using $C_{12}P^+I^-$ as the surfactant and attempted separation of the mixture into each phase. As a result, we found that the upper froth layer contained only pure Y and the remaining solid particles at the bottom of the funnel consisted of pure silica, as shown in panels B and C, respectively, of Figure 7. The X-ray powder diffraction patterns of the initial mixture, the floated particles, and the solid particles sunken at the bottom of the funnel further confirmed the high purity of each component (Figure 4 in the Supporting Information). It is also

(47) The gel composition was $SiO_2/NaAlO_2/NaOH/H_2O$ in a molar ratio of 1:0.2:0.6:12.

worth mentioning that less than 2 h was required to complete the separation, which otherwise would have taken at least several days by the conventional dissolution method. This result thus confirms that our standard method works equally well for the separation of real, autogenous reaction mixtures consisting of zeolite and silica.

Separation of an Autogenous Mixture of KL and an Unknown Zeolite into Each Component. We have long been interested in control of the morphology of KL (window size = 7.1 Å), stemming from our interest in the assembly of zeolite crystals on various supports.[48−54] Throughout our attempts to gain control over the morphology of the produced KL, we have found that the prepared gels often produce mixed phases of zeolite upon slight variations in the composition, aging time, reaction temperature, stirring procedure, etc., in the synthesis procedure. In some cases, we also observed a zeolite phase whose X-ray powder diffraction pattern did not match with any of the patterns listed in the *Collection of Simulated XRD Powder Patterns for Zeolites*.[55] The SEM image of the mixture revealed the presence of a species with nearly spherical morphology as well as cylindrical HL, as shown in Figure 7A. The unknown species retained its morphology even after repeated ion exchange of the autogenous cations with H^+. We then introduced the mixture (2 g) into a solution of $C_{12}P^+I^-$ (3 mM, 100 mL), and the solution was shaken for 3 min to generate froth. After settling for 30 min, the frothy solution underwent phase separation into three layers. The SEM image of the particles captured in the froth revealed the presence of the unknown species, as shown in Figure 7B. The SEM image of the particles that sank at the bottom of the funnel revealed that they consisted of only HL with a cylindrical morphology, as shown in Figure 7C. The X-ray powder diffraction patterns of the mixture, the floated unknown species, and the sunken HL further confirmed the high purity of each component (Figure 5 in the Supporting Information). The fact that $C_{12}P^+I^-$ can induce flotation of the unknown species even at such a low concentration allows us to predict that the species has an ion-exchange capacity. The above fact, coupled with the fact that the new species shows the first diffraction peak at relatively high angle (2 Å = 9.8), also suggests that the pore opening of the unknown species is smaller than the kinetic diameter of $C_{12}P^+$, i.e., 5.9 Å. We are currently taking the rigorous steps necessary for the confirmation and characterization of the new species. Of course, it is possible to analyze a new species even in mixed states with other known species. However, having the unknown species in the pure state will certainly facilitate its characterization and structural analysis with more credibility. In this regard, it can be said that our standard method can indeed be applied for the isolation of unknown zeolites from reaction mixtures for more facile and accurate structural analysis and characterization.

Conclusion

In summary, this report describes the surfactant-induced flotation of zeolite particles exchanged with M^{n+} with the aid of air bubbles. The dramatic change in the floated amount from a maximum to a minimum as the concentration shifts from slightly lower to slightly higher than the CMC is likened to the general behavior of froth flotation. Accordingly, it is proposed that hemimicelles are formed at concentrations below the CMC and admicelles are formed at the concentrations higher than the CMC on the external surfaces of the zeolites. In contrast, amorphous solids such as silica and alumina do not float under the same experimental conditions. The above two contrasting results serve as the experimental basis for applying this finding to the efficient separation of autogenous mixtures of an M^{n+}-exchanged zeolite and coprecipitated amorphous silica within 2 h, which otherwise would take several days if the conventional base treatment were applied. When M^{n+} ions are the charge-balancing cations in zeolites, the ion exchange between the surfactant cations and the charge-balancing cations preferentially occurs with the cations that reside on the external surfaces of the zeolites, even if the kinetic diameters of the surfactants are smaller than the sizes of the pore openings. However, the ion exchange occurs selectively with cations that reside in the interiors of the zeolites when H^+ is the charge-balancing cation, provided that the sizes of the pore openings do not restrict the access of the surfactant ions into the interiors of the zeolite crystals. As a result, unlike M^{n+}-exchanged zeolites, H^+-exchanged zeolites do not float when surfactants that can enter the zeolite pores are used. By applying the above results, the separation of an HMOR/H(90)Y mixture into each pure component was demonstrated by use of $C_{12}Q^+I^-$, which can be admitted only into H(90)Y but not into HMOR. However, this method is not suitable for the separation of basic zeolites such as zeolites P and X that decompose during acid exchange. This method also cannot be applied for the separation of mixtures of zeolites with very similar pore openings. It is also interesting to note that even zeolite particles with sizes well over 20 μm can be floated by surfactants (see Figure 7). Overall, this report describes the interesting effects of the nature of the charge-balancing cation and the pore size of the zeolites on the nature of the sorption of surfactant cations onto zeolites, which can be utilized as an experimental basis for the effective separation of zeolite/amorphous mixtures and even of mixtures of zeolites with different pore sizes into each pure component.

Acknowledgment. We thank the Ministry of Science and Technology (MOST), Korea, for supporting this work through the Creative Research Initiatives (CRI) program.

(48) Kulak, A.; Lee, Y.-J.; Park, Y. S.; Yoon, K. B. *Angew. Chem., Int. Ed.* **2000**, *39*, 950.
(49) Choi, S. Y.; Lee, Y.-J.; Park, Y. S.; Ha, K.; Yoon, K. B. *J. Am. Chem. Soc.* **2000**, *122*, 5201−5209.
(50) Ha, K.; Lee, Y.-J.; Lee, H. J.; Yoon, K. B. *Adv. Mater.* **2000**, *12*. 1114−1117.
(51) Lee, G. S.; Lee, Y.-J.; Ha, K.; Yoon, K. B. *Tetrahedron* **2000**, *56*, 6965−6968.
(52) Ha, K.; Lee, Y.-J.; Jung, D.-Y.; Lee, J. H.; Yoon, K. B. *Adv. Mater.* **2000**, *12*, 1614−1617.
(53) Kulak, A.; Park, Y. S.; Lee, Y.-J.; Chun, Y. S.; Ha, K.; Yoon, K. B. *J. Am. Chem. Soc.* **2000**, *122*, 9308−9309.
(54) Ha, K.; Lee, Y.-J.; Chun, Y. S.; Park, Y. S.; Lee, G. S.; Yoon, K. B. *Adv. Mater.* **2001**, *13*, 594−596.
(55) Treacy, M. M. J.; Higgins, J. B.; Ballmoos, R. *Collection of Simulated XRD Powder Patterns for Zeolites*, 3rd ed; Elsevier: New York, 1996.

Supporting Information Available: ^{1}H NMR data for the surfactant molecules synthesized in this work and X-ray diffraction patterns of fractions obtained from the separations of mixtures zeolites and amorphous materials and mixtures of zeolites with different pore sizes. This material is available free of charge via the Internet at http://pubs.acs.org.

CM0202097